bacteria; Clayton, R. K.; Sistrom, W. F., Ed.; Plenum Press: New York, U. S. A. 1978; p 349. (b) Gilman, P. B. *Photo. Sci. Eng.* **1978**, *18*, 418. (c) Wang, Y. *Chem. Phys. Lett.* **1986**, *126*, 209. (d) Liang, Y.; Ponte Goncalves, A. M.; Negus, D. K. *J. Phys. Chem.* **1983**, *87*, 1. (e) Liang, Y.; Ponte Goncalves, A. M. *J. Phys. Chem.* **1985**, *89*, 3290. (f) Anfinrud, P. A.; Causgrove, T. P.; Struve, W. S. *J. Phys. Chem.* **1986**, *90*, 5887. (g) Anfinrud, P. A.; Crackel, R. L.; Struve, W. S. *J. Phys. Chem.* **1984**, *88*, 5873. (h) Crackel, R. L.; Struve, W. S. *Chem. Phys. Lett.* **1985**, *120*, 473.

2. Arvan, Kh. L.; Zaitseva, N. E. *Opt. Spectrosc.* **1961**, *10*, 137.
3. (a) Valdes-Aguilera, O.; Neckers, D. C. *J. Phys. Chem.* **1988**, *92*, 4286. (b) Valdes-Aguilera, O.; Neckers, D. C. *Acc. Chem. Res.* **1989**, *22*, 171.
4. Sielcken, O. E.; van Tillborg, M.; Roks, M. F. M.; Hendriks, R.; Drenth, W.; Nolte, R. J. M. *J. Am. Chem. Soc.* **1987**, *109*, 4261.
5. West, W.; Pearce, S. *J. Phys. Chem.* **1965**, *69*, 1894.
6. (a) McRae, E. G.; Kasha, M. *J. Chem. Phys.* **1958**, *28*, 721. (b) McRae, E. G.; Kasha, M. In *Physical Processes in Radiation Biology*; Augenstein, L.; Rosenberg, B.; Mason, S. F., Ed.; Academic Press: New York, U. S. A. 1963.
7. Maeda, M. *Laser Dyes*; Academic Press: Tokyo, 1984.
8. Chen, S.-Y.; Horng, M.-L.; Quitevis, E. L. *J. Phys. Chem.* **1989**, *93*, 3683.
9. Emerson, E. S.; Conlin, M. A.; Rosenoff, A. E.; Norland, K. S.; Rodriguez, H.; Chin, D.; Bird, G. R. *J. Phys. Chem.* **1967**, *71*, 2396.
10. Graves, R. E.; Rose, P. I. *J. Phys. Chem.* **1975**, *79*, 746.
11. Kopainsky, B.; Hallermeier, J. K.; Kaiser, W. *Chem. Phys. Lett.* **1981**, *83*, 498.
12. Lax, M. *J. Chem. Phys.* **1952**, *20*, 1752.
13. Yu, J.; Berg, M. *J. Chem. Phys.* **1992**, *96*, 8741.
14. (a) Spano, F. C.; Mukamel, S. *Phys. Rev.* **1989**, *40*, 5783. (b). Carpenter, M. A.; Willand, C. S.; Penner, T. L.; Willwams, D. J.; Mukamel, S. J. *J. Phys. Chem.* **1992**, *96*, 2801. (c) Sasaki, F.; Kobayashi, S. *Appl. Phys. Lett.* **1993**, *63*, 2887.

A New Model for the Reduced Form of Purple Acid Phosphatase: Structure and Properties of $[Fe_2BPLMP(OAc)_2](BPh_4)_2$

Seon Hwa Yim, Ho Jin Lee, Kang-Bong Lee†, Seong Ju Kang†, Nam Hwi Hur‡, and Ho G. Jang*

Contribution from the Department of Chemistry, Korea University, Seoul 136-701, Korea
†Advanced Analysis Center, KIST, Seoul 136-130, Korea
†Department of Chemical Education, Korea National University of Education, Chungbuk 363-791, Korea
‡Korea Research Institute of Standards and Science, Taejon 305-600, Korea
Received February 12, 1998

$[Fe^{II}Fe^{III}BPLMP(OAc)_2](BPh_4)_2$ (**1**), a new model for the reduced form of the purple acid phosphatases, has been synthesized by using a dinucleating ligand, 2,6-bis[((2-pyridylmethyl)(6-methyl-2-pyridylmethyl)amino) methyl]-4-methylphenol (HBPLMP). Complex **1** has been characterized by X-ray diffraction method as having (μ-phenoxo)bis(acetato)diiron core. Complex **1** was crystallized in the monoclinic space group C2/c with the following cell parameters: a=41.620(6) Å, b=14.020(3) Å, c=27.007(4) Å, β=90.60(2)°, and Z=8. The iron centers in the complex **1** are ordered as indicated by the difference in the Fe-O bond lengths which match well with typical Fe^{III}-O and Fe^{II}-O bond lengths. Complex **1** has been studied by electronic spectral, NMR, EPR, SQUID, and electochemical methods. Complex **1** exhibits strong bands at 592 nm, 1380 nm in CH_3CN ($\varepsilon = 1.0\times10^3$, 3.0×10^2). These are assigned to phenolate-to-Fe^{III} and intervalence charge-transfer transitions, respectively. Its NMR spectrum exhibits sharp isotropically shifted resonances, which number half of those expected for a valence-trapped species, indicating that electron transfer between Fe^{II} and Fe^{III} centers is faster than NMR time scale. This complex undergoes quasireversible one-electron redox processes. The $Fe^{III}_2/Fe^{II}Fe^{III}$ and $Fe^{II}Fe^{III}/Fe^{II}_2$ redox couples are at 0.655 and −0.085 V *vs* SCE, respectively. It has $K_{comp}=3.3\times10^{12}$ representing that BPLMP/bis(acetate) ligand combination stabilizes a mixed-valence $Fe^{II}Fe^{III}$ complex in the air. Complex **1** exhibits a broad EPR signal centered near g=1.55 which is a characteristic feature of the antiferromagnetically coupled high-spin $Fe^{II}Fe^{III}$ system ($S_{total}=1/2$). This is consistent with the magnetic susceptibility study showing the weak antiferromagnetic coupling ($J=-4.6$ cm^{-1}, $H=-2JS_1\cdot S_2$) between Fe^{II} and Fe^{III} center.

Introduction

The purple acid phosphatases (PAP) constitute to a novel class of non-heme metalloenzymes which catalyze the hydrolysis of certain phosphate esters under weak acidic condition.[1] Although they have been isolated from a variety of

mammalian, plant, and microbial sources, only the PAP enzymes isolated from bovine spleen[2-8] and porcine uteroferrin[9-17] have been studied in some detail. Recently, a different PAP enzyme extracted from red kidney bean was reported having a heteronuclear FeZn unit in the active site.[18] However, the active sites of most PAPs contain dinuclear iron centers with two accessible oxidation states: a reduced active $Fe^{II}Fe^{III}$ form (PAP_{red}) and an oxidized inactive $Fe^{III}Fe^{III}$ form (PAP_{ox}).[1] The catalitically active $Fe^{II}Fe^{III}$ form (PAP_{red}) is pink (λ_{max}= 510 nm, ε=4000 $M^{-1}cm^{-1}$), while the catalytically inactive $Fe^{III}Fe^{III}$ form(PAP_{ox}) is purple (λ_{max}=560 nm, ε=4000 M^{-1} cm^{-1}).[4,9~11] These bands are assigned as tyrosinate-to-Fe^{III} charge transfer transitions which are confirmed by Resonance Raman study.[5] A distinctive feature of these proteins is the tyrosine residue bound to only one iron(III) center which contributes to similar extinction coefficients.[5]

The $Fe^{II}Fe^{III}$ form (PAP_{red}) exhibits rhombic EPR sigals at g=1.94, 1.73, and 1.58, which is consistent with an antiferromagnetically coupled high-spin $Fe^{II}Fe^{III}$ center.[6,11,12] In fact, magnetic susceptibility study shows that the Fe^{II} and Fe^{III} centers are weakly antiferromagnetically coupled with J values ranging from -5 to -11 cm^{-1} (where, $\boldsymbol{H}=-2J\mathbf{S}_1\cdot\mathbf{S}_2$).[5,14] Recent magnetic susceptibility study of the $Fe^{III}Fe^{III}$ form (PAP_{ox}) reveals a weak antiferromagnetic coupling ($J > -15$ cm^{-1}), which indicates lack of μ-oxo bridge.[8] X-ray structure and analysis has not been possible for the diiron PAP enzymes; however, EXAFS[7,15] and NMR[16] studies suggest that the iron center has an oxygen-rich coordination environment similar to that in ribonucleotide reductase.[19] It has been suggeted that iron centers are bonded to 3.5 N/O donors at about 2.14 Å, which are likely associated with histidine and aspartate or glutamate as well as a water molecule. A bridging hydroxo ligand has been suggested in the reduced form of the protein, but some controversy still exists on the nature of the bridging ligands at the oxidized center.

A number of recent model studies focused on the preparation of phenoxo-containing multidentate ligands having pyridine,[20,21] imidazole,[22] benzimidazole,[23] carboxylate,[24] and pyridine-phenolate[25~29] as pendant arms. However, it is still very important to investigate the controlling factor of stabilization of mixed-valence states and the characterization of the physical properties of mixed-valence complexes. Therefore, we have approached the subtle change in the structure by introducing the substituents to the dinucleating ligand and investigated the physical properties of those mixed-valence complexes. In this paper, we report the synthesis of the new dinucleating HBPLMP ligand and the crystal structure, spectral, magnetic, and electrochemical properties of the mixed-valence complex $[Fe^{II}Fe^{III}BPLMP(OAc)_2](BPh_4)_2$ (**1**) for a new model of the reduced form of the purple acid phosphatases.

Experimental Section

All reagents and solvents were purchased from commercial sources and used as received. Solvents were of either reagent or spectroscopic grade and were dried by standard procedures prior to use. 2,6-bis(chloromethyl)-4-methylphenol was prepared by following previously reported procedure.[20] Microanalyses were performed by Basic Science Research Center, Seoul.

(2-pyridylmethyl)(6-methyl-2-pyridylmethyl)amine (PLA). A mixture of 2-(aminomethyl)pyridine (1.2 g, 10 mmol) and 6-methyl-2-pyridinecaboxaldehyde (1.2 g, 10 mmol) in 60 mL of methanol was stirred for 3 hours at room temperature and 10% Pd/C (0.7 g) was added to the solution. The mixture was hydrogenated in a Parr hydrogenation apparatus at 40 psi at room temperature for 4 hours. The mixture was filtered and the filtrate was evaporated under reduced pressure. The product was purified by column chromatography (ethylacetate : ethanol=1 : 1) to afford a yellow oil (yield=80%). ^{1}H NMR ($CDCl_3$, δ): 2.54 (s, 3H, lutidyl-CH_3), 3.94, 3.99 (s, s, 2H, 2H, lutidyl-CH_2, pyridyl-CH_2), 7.02, 7.16, 7.37, 7.53, 7.65, 8.57 (d, d+t, d, t, t, d, 1H, 2H, 1H, 1H, 1H, 1H, lutidyl-*H*s and pyridyl-*H*s).

2,6-bis[((2-pyridylmethyl)(6-methyl-2-pyridylmethyl)amino)methyl]-4-methyl phenol (HBPLMP). This compound was synthesized by the literature method[21] with the following modification. Under N_2 atmosphere, a mixture of (2-pyridylmethyl)(6-methyl-2-pyridylmethyl)amine (4.2 g, 20 mmol) and triethylamine (2.0 g, 20 mmol) in 15 mL of THF was added dropwise to a stirred THF solution of 2,6-bis(chloromethyl)-4-methylphenol (2.0 g, 10 mmol) at O °C. When the addition was completed, the mixture was allowed to warm to room temperature. After 3 days, the stirred mixture was filtered to remove triethylammonium salts, and the filterate was concentrated under reduced pressure. The residue was dissolved in 40 mL of water, and the product was extracted with three 40 mL portions of methylene chloride. The extracts was washed with brine, and dried over anhydrous $MgSO_4$. The product was purified by column chromatography to afford 4.5 g (80% yield) of a yellow oil. FAB$^+$-Mass m/z: 559 ($M-H^+$), Anal. Calcd for $C_{35}H_{38}N_6O$: C, 75.20; H, 6.85; N, 15.00. Found: C, 75.28; H, 7.37; N, 15.13. ^{1}H NMR ($CDCl_3$, δ) 2.23 (s, 3H, Ar-CH_3), 2.53 (s, 6H, lutidyl-CH_3), 3.76 (s, 4H, Ar-CH_2), 3.83, 3.86 (s, s, 4H, 4H, lutidyl-CH_2, pyridyl-CH_2), 6.98, 7.01, 7.31, 7.50, 7.56, 7.60, 8.51 (d+d, t, d, d, d, t, d, 4H, 2H, 2H, 2H, 2H, 2H, 2H, lutidyl-*H*s and pyridyl-*H*s). 10.70 (b, 1H, Ar-*OH*).

$[Fe^{II}Fe^{III}BPLMP(OAc)_2](BPh_4)_2$ (1). A solution of 0.21 g (0.38 mmol) of HBPLMP in 10 mL methanol was treated with a solution of 0.31 g (0.76 mmol) of $Fe(NO_3)_3\cdot 9H_2O$ in 5 mL of methanol to yield a dark-green solution. Addition of 0.094 g (1.14 mmol) of sodium acetate in 4 mL of methanol caused the formation of dark blue-green solution. After 30 min stirring at room temperature, metathesis with 0.29 g (0.84 mmol) of sodium tetraphenylborate resulted in the immediate precipitation of the bluish-green crude product. Further purification was achieved by recrystallization of the crude product by vapor diffusion of methanol into an acetone solution of **1** to afford dark blue-green crystals. FAB$^+$-Mass m/z: 787 (M^{2+}), Anal. Calcd for $C_{87}H_{83}B_2Fe_2N_6O_5$: C, 73.30; H, 5.87; N, 5.90. Found: C, 72.80; H, 6.24; N, 5.80.

Physical Measurements

^{1}H NMR spectra were obtained on Varian Unity plus 300 and Unity plus 600 spectrometers. The paramagnetic ^{1}H NMR spectra were obtained using a 90° pulse with 16 K data points. An inversion-recovery pulse sequence (180°-τ-90°-AQ) was used to obtain non-selective proton relaxation

times (T_1). A typical magnitude ^{1}H-COSY spectrum was collected with 1024 data points in t_2 and 256 data points in t_1 with a band width of 10 kHz and a repetition time of < 0.2 s. The time for the data collection for a ~10 mM sample was about 8 hrs. A zero-degree shifted sine bell was applied in both dimensions and zero-filled to 2048 $t_2 \times 2048$ t_1 data points prior to Fourier transformation and symmetrization. In this study, cross signals from pairs of signals with $\Delta\delta < 1$ ppm in a spectral width of ~30 ppm could be clearly recognized under proper processing procedures. Electronic spectra were measured on an Hewlett-Packard 8452A diode array spectrometer. Near-IR spectrum was recorded with Varian Cary 17DX spectrophotometer. FAB Mass spectrum was performed on VG70-VSEQ (VG Analytical, UK). X-band EPR measurements were performed with Bruker ESP-300S spectrometer equipped with an Oxford liquid helium cryostat. Magnetic susceptibility measurements was performed with SQUID Quantum Design II susceptometer. Electrochemical studies are performed with a BAS 51W electrochemical analyzer (Biochemical Systems, Inc., West Lafayette, IN). All electrochemical experiments were done under argon at ambient temperature in solutions of acetonitrile with 0.1 M tetrabutylammonium perchlorate as the supporting electrolyte. Cyclic voltammograms were obtained by using a three-component system consisting of a platinum net working electrode, a platinum wire auxiliary electrode, and a BAS Ag/Ag^+ or saturated calomel reference electrode containing a Vycore tip plug to separate it from the bulk solution. The ferrocinium/ferrocene couple was used to monitor the reference electrode.

X-ray crystallography

A dark blue-green crystal of $[Fe^{II}Fe^{III}BPLMP(OAc)_2](BPh_4)_2$ (**1**), (dimensions: $0.50 \times 0.40 \times 0.15$ mm) was mounted on the Enraf-Nonius CAD4 automatic diffractometer with graphite-monochromated Mo Kα (λ=0.71073 Å) at ambient temperature. The cell dimensions were obtained by least-squares refinements of the setting angles for 25 well-centered reflections. The data were corrected for Lorentz and polarization effects. Absorption effects were corrected by the empirical psi-scan method. The structure was solved by Patterson methods (SHELXS-86), and was refined by full-matrix least squares technique (SHELXS-93). The crystallographic and refinement data are summarized in Table 1. All non-H atoms were refined with anisotropic thermal parameters. Hydrogen atoms were included in the structure factor correlation in idealized positions (d(C-H)=0.95 Å, BH=3.0). The weighting scheme was based on counting statistics and included a factor (p=0.05) to downweight the intense reflections. The maximum and minimum peaks on the final difference Fourier map correspond to 1.325 and −1.047 e/Å^3, respectively. An ORTEP plot of the structure of the cation is shown in Figure 1, together with the numbering scheme for the complex. Selected bond lengths and bond angles are listed in Table 2, while atomic coordinates, thermal parameters, and a complete listing of bond lengths and angles are available as supplementary material.

Results and Discussion

Description of the X-ray structure of $[Fe^{II}Fe^{III}$

Table 1. Crystallographic Data and Structure Refinement for **1**

formula	$C_{87}H_{83}B_2Fe_2N_6O_5$
FW	1425.91
T (°C)	20
wavelength, Å	0.71073
space group	C2/c
a, Å	41.620(6)
b, Å	14.020(3)
c, Å	27.007(4)
β, deg	90.60(2)
V, Å^3	15758(6)
Z	8
ρ_{calcd}, gm^{-3}	1.202
μ(Mo Kα), cm^{-1}	4.23
no. of rflns collctd	4560
no. of indep rflns	4490 [R(int)=0.0242]
no. of params	919
GOF on F^2	1.210
final R indices [$I > 2\sigma(I)$]	R1[a]=0.0689, wR2=0.1652
R indices (all data)	R1=0.0770, wR2=0.1713
largest diff. peak and hole, e/Å^3	+0.657 and −0.216

[a] $R1 = \Sigma \| F_o \| - \| F_c \| / \Sigma \| F_o \|$. $wR2 = \{\Sigma w(F_o^2 - F_c^2)^2 / \Sigma w F_o^4\}^{1/2}$, where $w = 1/\{\sigma^2 F_o^2 + (0.0786P)^2 + 5.28P\}$ and where $p = \{\text{Max}(F_o^2, 0) + 2F_c\}/3$.

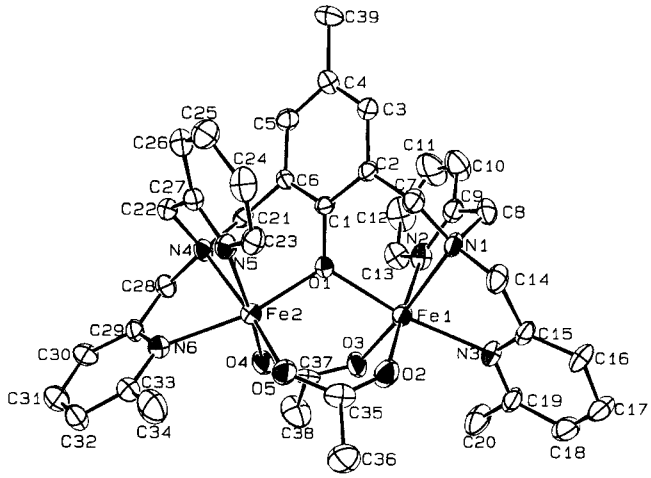

Figure 1. Structure of the cation of **1**, showing the atom-labeling scheme. Important bond lengths (Å) and angles (°): Fe_1O_1= 2.110(7), Fe_2-O_1=1.964(7), $Fe_1 \cdots Fe_2$=3.473(7), Fe_1-O_1-Fe_2=116.9(4).

$BPLMP(OAc)_2](BPh_4)_2$ (1). Complex **1** crystallizes in the monoclinic space group C2/c. The structure of the cation of **1** is shown in Figure 1, and selected bond lengths and angles are given in Table 2. The structure of **1** reveals that the iron centers are triply bridged by an oxygen atom from a phenolate and by two acetate ligands, thus giving what increasingly appears to be a thermodynamically favored core structure. The remaining coordination sites of each iron centers are occupied by nitrogen atoms from amine, pyridyl, and 6-methylpyridyl pendants, resulting distorted octahedral geometries. Though the iron centers in **1** are coordinated by a N_3O_3 donor set, it shows significant differences in the Fe-O bond lengths for the two Fe centers (2.110 and 1.964 Å), which match well with Fe^{II}-O and Fe^{III}-O bond lengths of the known complexes.[20-23] The Fe^{II}-O_1 and Fe^{III}-O_1 bond distances in **1** are slightly longer than

Table 2. Selected Bond Lengths (Å) and Angles (deg) for **1**

Fe(1)-O(1)	2.110(7)	Fe(1)-O(2)	2.118(9)
Fe(1)-O(3)	2.042(8)	Fe(1)-N(1)	2.205(8)
Fe(1)-N(2)	2.140(10)	Fe(1)-N(3)	2.179(9)
Fe(2)-O(1)	1.964(7)	Fe(2)-O(4)	1.987(8)
Fe(2)-O(5)	1.926(8)	Fe(2)-N(4)	2.180(8)
Fe(2)-N(5)	2.135(9)	Fe(2)-N(6)	2.201(9)
O(1)-Fe(1)-O(2)	89.5(3)	O(1)-Fe(1)-O(3)	90.1(3)
O(2)-Fe(1)-O(3)	93.1(4)	O(1)-Fe(1)-N(1)	86.9(3)
O(2)-Fe(1)-N(1)	96.7(4)	O(3)-Fe(1)-N(1)	169.7(3)
O(1)-Fe(1)-N(2)	90.8(3)	O(2)-Fe(1)-N(2)	175.6(4)
O(3)-Fe(1)-N(2)	91.3(4)	O(1)-Fe(1)-N(3)	159.3(3)
O(2)-Fe(1)-N(3)	80.8(3)	O(3)-Fe(1)-N(3)	108.5(4)
N(1)-Fe(1)-N(2)	78.9(4)	N(1)-Fe(1)-N(3)	76.3(4)
N(2)-Fe(1)-N(3)	97.5(3)	O(1)-Fe(2)-O(4)	94.2(3)
O(1)-Fe(2)-O(5)	98.0(3)	O(4)-Fe(2)-O(5)	95.5(3)
O(1)-Fe(2)-N(4)	89.1(3)	O(4)-Fe(2)-N(4)	90.9(3)
O(5)-Fe(2)-N(4)	170.0(3)	O(1)-Fe(2)-N(5)	87.5(3)
O(4)-Fe(2)-N(5)	169.9(4)	O(5)-Fe(2)-N(5)	94.2(4)
O(1)-Fe(2)-N(6)	163.8(4)	O(4)-Fe(2)-N(6)	84.9(3)
O(5)-Fe(2)-N(6)	98.2(4)	N(4)-Fe(2)-N(5)	79.1(4)
N(4)-Fe(2)-N(6)	74.8(4)	N(5)-Fe(2)-N(6)	90.7(3)
C(1)-O(1)-Fe(1)	119.3(6)	C(1)-O(1)-Fe(2)	123.6(6)
Fe(1)-O(1)-Fe(2)	116.9(4)	C(35)-O(2)-Fe(1)	134.6(9)
C(37)-O(3)-Fe(1)	137.0(8)	C(37)-O(4)-Fe(2)	133.7(8)
C(35)-O(5)-Fe(2)	132.9(8)	C(7)-N(1)-C(8)	111.4(9)

those (2.090 and 1.943 Å) of $[Fe^{II}Fe^{III}BPMP(OPr)_2](BPh_4)_2$ (**2**).[21] The structure of **1** is confirmed as the mixed-valence nature of this dinuclear complex by exhibiting discrete Fe^{II} and Fe^{III} centers. Interestingly, both nitrogen atoms of 6-methylpyridyl ring are trans to oxygen atom of bridged phenolate and are pointing down and away each other. The Fe_1-N_3 and Fe_2-N_6 bond distances in the complex **1** are longer than those of the complex **2**. In addition, the bond angle Fe-O-Fe is also bigger than that of $[Fe^{II}Fe^{III}BPMP(OPr)_2](BPh_4)_2$ (**2**), $[Fe^{II}Fe^{III}BIMP(OAc)_2](BPh_4)_2$ (**3**), and $[Fe^{II}Fe^{III}BZIMP(OAc)_2](BPh_4)_2$ (**4**).[20-23] These results are presumably due to the steric effect of the methyl substituents on the pyridine ring.[30] In the previous (μ-phenoxo) diiron complexes **2**, **3**, and **4** with similar triply bridged cores, the metal-metal separation is constrained by the carboxylate bridges to be less than 3.45 Å. However, the Fe-Fe distance in the complex **1** of 3.473 Å is longer than those of previous (μ-phenoxo)mixed-valence complexes **2**, **3**, and **4** and is comparable to 3.52 Å distance found in the reduced form of uteroferrin by EXAFS study.[15]

Table 3. Isotropic shifts and experimental relaxation times of **1**

Peak	Chemical shift (ppm)	T_{1exp} (ms)
$CH_2(A_e)$	368	nd
$CH_2(A_a)$	77	0.8
$CH_2(B_e)$	176	3.3
$CH_2(B_a)$	43	1.3
$CH_2(C_e)$	266	10
$CH_2(C_a)$	47	0.9
β_1	78	17
γ	12	30
$_1CH_3$	21.5	13
α	−25	3.1
β_1'	176	3.3
γ'	74	15
β_2'	0.5	nd

Greek letters designate positions of pyridyl rings.

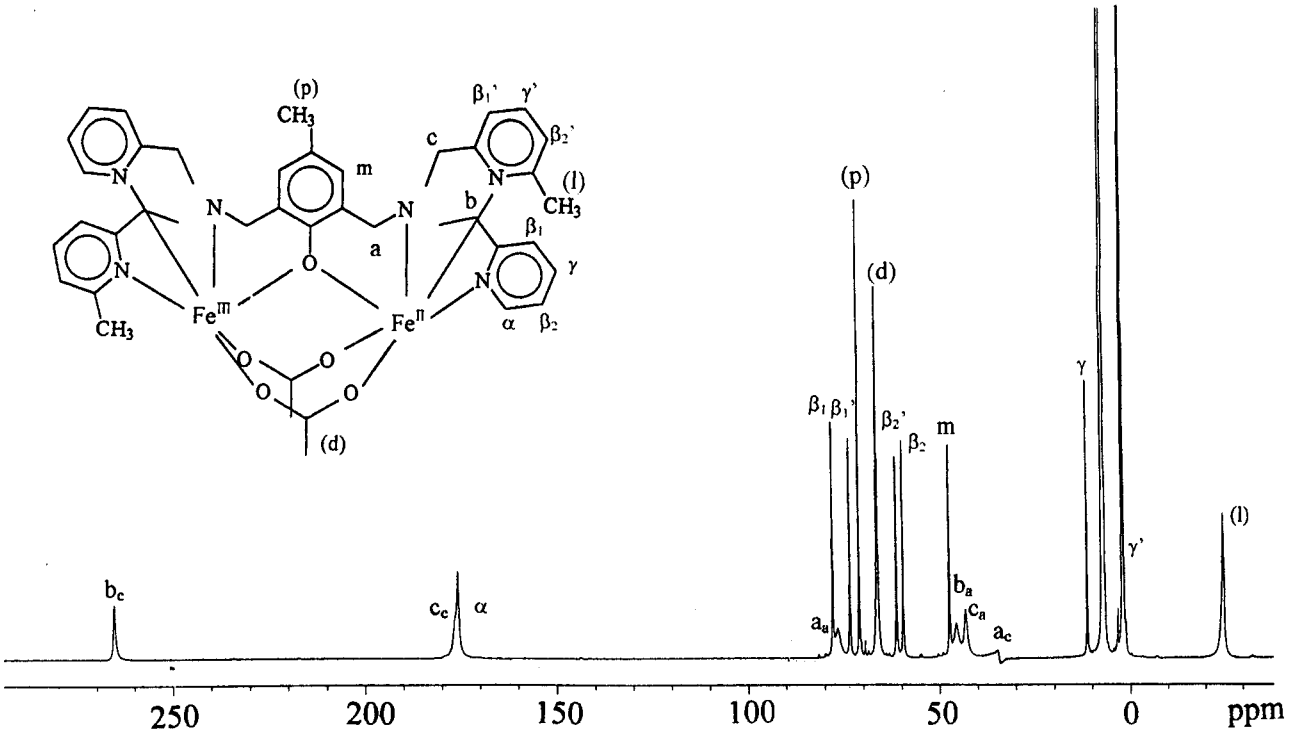

Figure 2. ^1H NMR spectrum of **1** in CD_3CN.

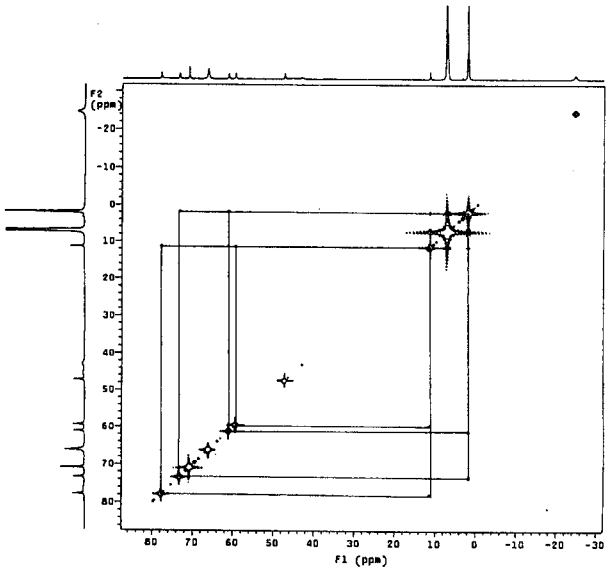

Figure 3. COSY spectrum of **1** in CD_3CN.

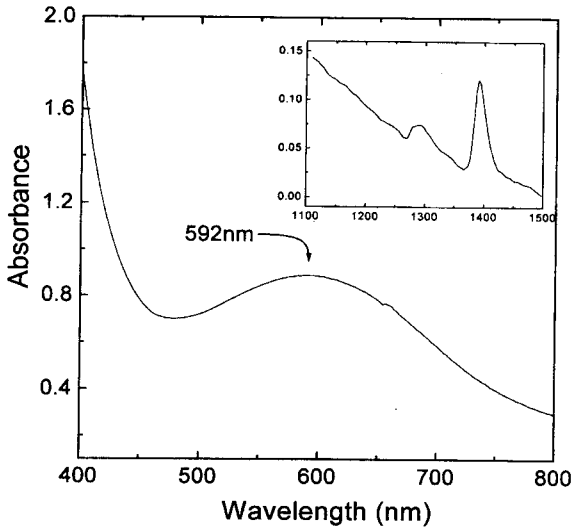

Figure 4. Visible absorption spectrum of **1** in CH_3CN at ambient temperature. Inset: near IR spectrum of **1** in CH_3CN.

^{1}H NMR studies

^{1}H NMR spectroscopy has been established as a useful probe of the structural and magnetic properties of the mixed-valence complexes.[31] The NMR spectrum of the complex **1** displays relatively sharp well-resolved resonances that span 350 ppm range in chemical shift. The narrow line widths of the signals are consistent with the diiron (II, III) complex adopting the T_{1e} of the fast electonic relaxation high-spin Fe^{II} center (Figure 2).[32] Most of protons can be assigned by comparison of integration, T_1 values (Table 3), and COSY connectivities (Figure 3).

All twelve CH_2 protons appear as six resonances (A_e, B_e, C_e, A_a, B_a, C_a) with very short T_1 values and two-proton integrations each; the number of resonances observed suggests that there is a two-fold axis symmetry relating the two halves of the molecule. It is noted that A_e (365 ppm) peak is folded and appears at 35 ppm due to the limit of spectral width. Thus, the six CH_2 resonances would arise in the half-molecule from the two protons on the phenolate backbone and the four protons associated with the pyridyl arms. The COSY spectrum of **1** (Figure 3) shows several cross peaks of the pyridyl (β_1', β_2', γ') and 6-methylpyridyl (β_1, β_2, γ) pendants present in the complex. However, α protons of the pyridyl ring being too close to the metal centers have T_1 values too short to permit its connectivity to the corresponding β protons to be observed; we assign them to remaining unassigned features with appropriately T_1 values. Also, the CH_3 proton peak of the 6-methylpyridine is observed at -25 ppm with short T_1 value. In addition, the CH_3 protons of the bound acetate and CH_3 protons of the bridged phenolate were found at 71 ppm and 66 ppm, respectively, similar to those of $[Fe^{II}Fe^{III}BPMP(OPr)_2](BPh_4)_2$.[21]

The analysis of the assignments reveals that only 17 distinct signals are observed, indicating that electron transfer between the metal centers is faster than the NMR time scale and thus, there is a two-fold axis symmetry relating the two halves of the molecule in the solution. Therefore, complex **1** is valence-detrapped and belongs to the class II mixed-valence complex according to the Robin-Day classification.[33]

Electronic Absorption Spectra

$[Fe^{II}Fe^{III}BPLMP(OAc)_2](BPh_4)_2$ (**1**) is air-stable bluish green solid. Complex **1** exhibits strong absorption band at 592 nm in CH_3CN ($\varepsilon=1.0\times10^3$) as shown in Figure 4. This band is due to the charge transfer transition from filled $p\pi$ orbitals of phenolate oxygen to the half filled $d\pi^*$ orbitals of the Fe^{III} center. All the (μ-phenoxo)mixed-valence complexes display phenolate-to-Fe(III) charge transfer transition. For example, similar charge transfer bands are observed at 523, 554, and 570 nm for $[Fe^{II}Fe^{III}BPMP(OPr)_2](BPh_4)_2$,[21] $[Fe^{II}Fe^{III}$-$BIMP(OAc)_2](BPh_4)_2$,[22] and $[Fe^{II}Fe^{III}BZIMP(OAc)_2](BPh_4)_2$,[23] respectively. Interestingly, complex **1** also exhibits a broad band at 1380 nm ($\varepsilon=3.0\times10^2$) in the near-IR region. Since diferrous and diferric complexes do not show any near-IR bands, it can be assigned to intervalence charge-transfer transition which is a characteristic of mixed-valence complex.[34]

Electrochemistry

Cyclovoltammogram of complex **1** in acetonitrile is shown in Figure 5. Complex **1** displays two quasireversible one-electron redox processes corresponding to the $Fe^{III}{}_2$/$Fe^{II}Fe^{III}$ and $Fe^{II}Fe^{III}$/$Fe^{II}{}_2$ couples at 0.655 and -0.085 V *vs.* SCE, respectively. These values are slightly shifted to negative potential than that of $[Fe^{II}Fe^{III}BPMP(OAc)_2](BPh_4)_2$.[20] This slightly cathodic shifted potential of complex **1** reflects the effect of electron-donating ability of methyl substituents of the 6-methylpyridine rings.

We have determined the thermodynamic stability of the mixed-valence form by evaluating its comproportionation constant (K_{comp}) for the equilibrium;

$$[Fe^{III}{}_2BPLMP(OAc)_2]^{3+} + [Fe^{II}{}_2BPLMP(OAc)_2]^{+} \overset{K_{comp}}{\rightleftharpoons} 2[Fe^{II}Fe^{III}BPLMP(OAc)_2]^{2+} \quad (1)$$

$$\Delta E = (RT/nF)\ \ln K_{comp} \quad (2)$$

The large value of ΔE (0.74 V) of complex **1** yields $K_{comp}=3.3\times10^{12}$ which indicates a substantial stability of the $Fe^{II}Fe^{III}$ complex over its corresponding $Fe^{II}{}_2$ or $Fe^{III}{}_2$ complexes. Interestingly, the comproportionation constant of complex **1** is slightly larger than those of reported phenoxo-bridged complexes, $[Fe^{II}Fe^{III}BPMP(OPr)_2]^{2+}$ ($K_{comp}=7.5\times10^{11}$)

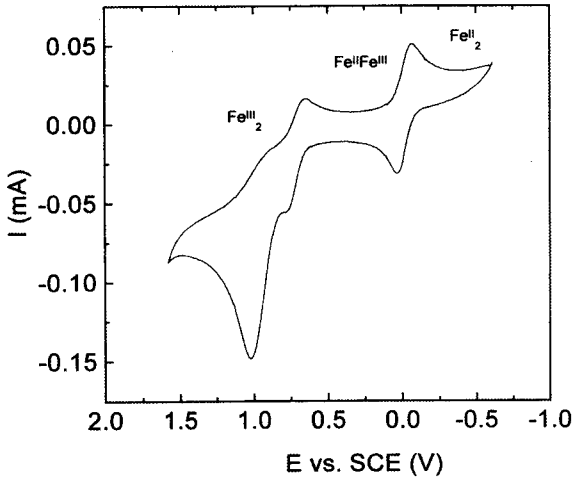

Figure 5. Cyclic voltammogram of complex **1** versus SCE in CH_3CN with 0.1 M $TBAClO_4$ under argon using a 100 mV/sec scan rate. The reversible oxidative wave near 1000 mV is due to the oxidation of the BPh_4 counter anion.

and $[Fe^{II}Fe^{III}BIMP(OAc)_2]^{2+}$ ($K_{comp}=1\times10^{11}$).[21,22] The structural effects, and Coulombic interactions are the most probable factors that determine the different stabilization for complex **1** when compared with $[Fe^{II}Fe^{III}BPMP(OPr)_2]^{2+}$.[35]

Magnetic properties

EPR spectroscopy has been very useful for characterizing the diiron (II, III) centers in the dinuclear metal complexes and proteins.[36] These centers exhibit a signal with $g_{av}<2.0$, which is indicative of antiferromagnetic coupling between high-spin Fe^{III} ($S_1=5/2$) and high-spin Fe^{II} ($S_2=2$), resulting in an $S_{total}=1/2$ ground state.[37] Complex **1** exhibits a broad intense EPR signal centered near g=1.55 with very weak signals at g=4.3 (Figure 6). A similar broad signal near g=1.6 has also been reported in $[Fe^{II}Fe^{III}BPMP(OPr)_2]^{+}$ complex.[21]

In order to understand the magnetic property of complex **1**, the variable-temperature magnetic susceptibility data of **1** in the solid state, collected in the temperature range 5-195 K, were obtained (Figure 7). The plot shows typical process

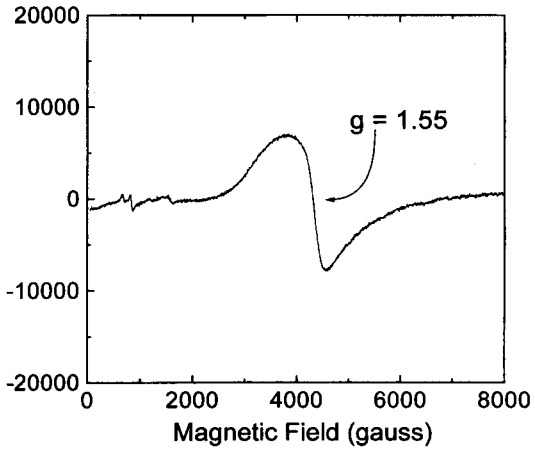

Figure 6. EPR spectrum of a frozen solution of **1** in CH_3CN at 4 K. Instrumental parameters: microwave frequency, 9.42 GHz; power, 5 mW; modulation frequency, 100 kHz; modulation amplitude, 5.08; gain, 2.5×10^4.

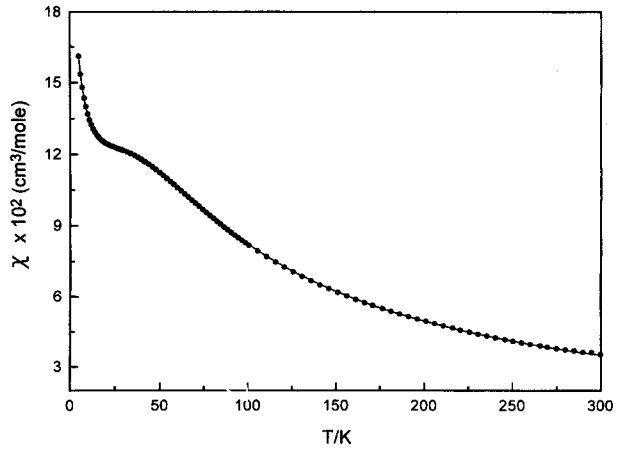

Figure 7. Plot of the magnetic susceptibility of powder sample as functions of temperature for **1**. The solid line resulted from a least-squares fit of the data.

of antiferromagnetically coupled system. The data were fitted by using the expression for molar susceptibility versus temperature from the following spin Hamiltonian[38]:

$$\boldsymbol{H}=-2JS_1\cdot S_2+\sum[D_i(S_{zi}^2-\tfrac{1}{3}S_i(S_i+1))+E_i(S_{\xi}^2-S_{yi}^2)+\beta S_i\cdot g_i\cdot H] \quad (3)$$

where, J is the isotropic exchange coulping constant, S_i denotes spin state ($S_1=2$ and $S_2=5/2$), and D_i and E_i are the axial and rhombic zero-field splitting parameters. The final parameter set of the best fit was found to be $J=-4.6$ cm^{-1}, $g_1=2.02$, $D_1=-9.27$ cm^{-1}, $g_2=2.00$ (fixed), and $D_2=0.00$ cm^{-1} (fixed) with $E_1/D_1=0.113$ and $E_2/D_2=0.333$. The coupling constant for **1** ($J=-4.6$ cm^{-1}) consistents with the EPR data and represents the typical range for μ-phenoxo or μ-alkoxo bridged diiron (II, III) system with a weak antiferromagnetic coupling.[21-29] Magnetic susceptibility result is consistent with the EPR data of **1**.

Summary

we have synthesized and characterized $[Fe^{II}Fe^{III}BPLMP(OAc)_2](BPh_4)_2$ (**1**), as a new model of the reduced form of the purple acid phosphatases, in order to investigate the effect of the subtle change in the structure by introducing the substituents to the dinucleating ligand. Complex **1** exhibits the quite interesting features in terms of structural and physical properties due to the steric effect of the methyl substituents on the pyridine ring.

The analysis of the NMR assignments reveals that the electron transfer between the metal centers is faster than the NMR time scale. Complex **1** exhibits a broad EPR signal centered near g=1.55 which is a characteristic feature of the antiferromagnetically coupled high-spin $Fe^{II}Fe^{III}$ complex. The magnetic susceptibility study shows the weak antiferromagnetic coupling ($J=-4.6$ cm^{-1}) between Fe^{II} and Fe^{III} center. As a result, complex **1** is valence-detrapped and belongs to the class II mixed-valence complex according to the Robin-Day classification. Therefore, the dependence of the physical properties on the bridging and terminal ligands in the model complexes should provide important insights into the magnetic and electronic interaction of such dinuclear iron centers surrounded with hydrophobic packet amino acid residues in biological systems. The studies of the

phosphate binding ability of complex **1** and its reactivity are in progress in our laboratory and will be the subject of future reports.

Acknowledgment. This work has been supported by the Korea Science and Engineering Foundation (Grant No. 96-0501-01-01-3) and the Basic Science Research Institute Program (Project No. BSRI-97-3407).

Supplementary Material Available: Tables of atomic coordinates, equivalent Isotropic displacement parameters, complete bond lengths and bond angles for $[Fe^{II}Fe^{III}BPLMP(OAc)_2](BPh_4)_2$ (**1**). Ordering information is given on any current masthead page.

References

1. For recent reviews of these enzymes, see: (a) Sanders-Loehr, J. in *Iron Carriers and Iron Proteins*; Loehr, T. M., Ed.; VCH Publishers: New York, 1989; Vol. 5, 373-466. (b) Que, L., Jr.; True, A. E. *Prog. Inorg. Chem.* **1990**, *38*, 97-200. (c) Vincent, J. B.; Oliver-Lilley, G. L.; Averill, B. A. *Chem. Rev.* **1990**, *90*, 1447-1467. (d) Anderson, K. K.; Grüslund, A. *Advances in Inorganic Chemistry*, **1995**, *43*, 359-408. (e) Wilcox, D. E. *Chem. Rev.* **1996**, *96*, 2435-2458.
2. Davis, J. C.; Lin, S. S.; Averill, B. A. *Biochemistry* **1981**, *20*, 4062-4067.
3. Antanaitis, B. C.; Aisen, P. *J. Biol. Chem.* **1982**, *257*, 1855-1859.
4. (a) Antanaitis, B. C.; Aisen, P. *Adv. Inorg. Biochem.* **1983**, *5*, 111-136. (b) Antanaitis, B. C.; Strekas, T.; Aisen, P. *J. Biol. Chem.* **1982**, *257*, 3766-3770.
5. Averill, B. A.; Davis, J. C.; Burman, S.; Zirino, T.; Sanders-Loehr, J.; Loehr, T. M.; Sage, J. T.; Debrunner, P. G. *J. Am. Chem. Soc.* **1987**, *109*, 3760-3767.
6. Dietrich, M.; Münsternmann, D.; Suerbaum, H.; Witzel, H. *Eur. J. Biochem.* **1991**, *199*, 105-113.
7. Kauzlarich, S. M.; Teo, B. K.; Zirino, T.; Burman, S.; Davis. J. C.; Averill, B. A. *Inorg. Chem.* **1986**, *25*, 2781-2785.
8. Crowder, M. W.; Vincent, J. B.; Averill, B. A. *Biochemistry* **1992**, *31*, 9603-9608.
9. Antanaitis, B. C.; Aisen, P. *J. Biol. Chem.* **1984**, *259*, 2066-2069.
10. Lim, J. S.; Manuel, A. S.; Sykes, A. G. *Inorg. Chem.* **1996**, *35*, 614-618.
11. Antanaitis, B. C.; Aisen, P.; Lilienthal, H. R. *J. Biol. Chem.* **1983**, *258*, 3166-3172.
12. Davis, S. S.; Que, L., Jr. *J. Am. Chem. Soc.* **1990**, *112*, 6455-6463.
13. Pyrz, J. W.; Sage, J. T.; Debrunner, P. G.; Que, L., Jr. *J. Biol. Chem.* **1986**, *261*, 11015-11020.
14. Day, E. P.; David, S. S.; Peterson, J.; Dunham, W. R. Bonvoison, J. J.; Sands, R. H.; Que, L., Jr. *J. Biol. Chem.* **1988**, *263*, 15561-15567.
15. True, A. E.; Scarrow, R. C.; Randall, C. R.; Holz, R. C.; Que, L., Jr. *J. Am. Chem. Soc.* **1993**, *115*, 4246-4255.
16. (a) Lauffer, R. B.; Antanaitis, B. C.; Aisen, P.; Que, L., Jr. *J. Biol. Chem.* **1983**, *258*, 14212-14218. (b) Scarrow, R. C.; Pyrz, J. W.; Que, L., Jr. *J. Am. Chem. Soc.* **1990**, *112*, 657-665. (c) Wang, Z.; Ming, L. J.; Que, L., Jr. *Biochemistry* **1992**, *31*, 5263-5268.
17. Crans, D. C.; Simone, C. M.; Holz, R. C.; Que, L., Jr. *Biochemistry.* **1992**, *31*, 11731-11739.
18. Sträter, N.; Klabunde, T.; Tucker, P.; Witzel, H.; Krebs, B. *Science* **1995**, *268*, 1489.
19. (a) Nordlund, P.; Sjoberg, B. M.; Eklund, H. *Nature* **1990**, *345*, 593-598. (b) Wallar, B. J.; Lipscomb, J. D. *Chem. Rev.* **1996**, *96*, 2625-2657.
20. Suzuki, M.; Uehara, A.; Oshio, H.; Endo, K.; Yanaga, M.; Kida, S.; Saito, K. *Bull. Chem. Soc. Jpn.* **1987**, *60*, 3547-3555.
21. (a) Borovik, A. S.; Que, L., Jr. *J. Am. Chem. Soc.* **1988**, *110*, 2345-2347. (b) Borovik, A. S.; Papaefthymiou, V.; Taylor, L. F.; Anderson, O. P.; Que, L., Jr. *J. Am. Chem. Soc.* **1989**, *111*, 6183-6195.
22. (a) Mashuta, M. S.; Webb, R. J.; McCusker, J. K.; Schmitt, E. A.; Oberhausen, K. J.; Richardson, J. F.; Buchanan, R. M.; Hendrickson, D. N. *J. Am. Chem. Soc.* **1992**, *114*, 3815-3827. (b) Mashuta, M. S.; Webb, R. J.; Oberhausen, K. J.; Richardson, J. F.; Buchanan, R. M.; Hendrickson, D. N. *J. Am. Chem. Soc.* **1989**, *111*, 2745-2746.
23. Suzuki, M.; Oshio, H.; Uehara, A.; Endo, K.; Yanaga, M.; Kida, S.; Saito, K. *Bull. Chem. Soc. Jpn.* **1988**, *61*, 3907-3913.
24. Borovik, A. S.; Murch, B. P.; Que, L., Jr.; Papaefthymiou, V.; Münck, E. *J. Am. Chem. Soc.* **1987**, *109*, 7190-7191.
25. (a) Neves, A.; Erthal, S. M. D.; Drago, V.; Griesar, K.; Haase, W. *Inorg. Chim. Acta.* **1992**, *197*, 121-124. (b) Neves, A.; de Brito, M. A.; Vencato, I.; Drago, V.; Griesar, K.; Haase, W.; Mascarenhas, Y. P. *Inorg. Chem.* **1996**, *35*, 2360-2368.
26. Neves, A.; de Brito, M. A.; Vencato, I.; Drago, V.; Griesar, K.; Hasse, W. *Inorg. Chim. Acta.* **1993**, *214*, 5-8.
27. Neves, A.; de Brito, M. A.; Drago, V.; Griesar, K.; Haase, W. *Inorg. Chim. Acta.* **1995**, *237*, 131-135.
28. Krebs, B.; Schepers, K.; Bremer, B.; Henkel, G.; Althaus, E.; Müller-Warmuth, W.; Griesar, K.; Haase, W. *Inorg. Chem.* **1994**, *33*, 1907-1914.
29. Nie, H.; Aubin, S. M. J.; Mashuta, M. S.; Wu, C. C.; Richardson, J. F.; Hendrickson, D. N.; Buchanan, R. M. *Inorg. Chem.* **1995**, *34*, 2382-2388.
30. Zang, Y.; Kim, J.; Dong, Y.; Wilkinson, E. C.; Appelman, E. H.; Que, L., Jr. *J. Am. Chem. Soc.* **1997**, *119*, 4197-4205.
31. Ming, L. J.; Jang, H. G.; Que, L., Jr. *Inorg. Chem.* **1992**, *31*, 359-364.
32. Bertini, I.; Luchinat, C. *NMR of Paramagnetic Molecules in Biological Systems*; The Benjamin/Cummings Publishing Company, Inc. California 1986.
33. Robin, M. B.; Day, P. *Adv. Inorg. Chem. and Radiochem.* **1967**, *10*, 247-422.
34. Creutz, C. *Prog. Inorg. Chem.* **1983**, *30*, 1-73.
35. Gagnè, R. R.; Spiro, C. L.; Smith, T. J.; Hamann, C. A.; Thies, W. R.; Shuemke, A. K. *J. Am. Chem. Soc.* **1981**, *103*, 4073-4081.
36. Wertz, J. E.; Bolton, J. R. in *Electron Spin Resonance: Elementary Theory and Practical Applications*; McGraw-Hill, Inc.: 1972.
37. Münck, E.; Debrunner, P. G.; Tsibris, J. C. M.; Gunsalus, I. C. *Biochemistry* **1972**, *11*, 855-863.
38. Day, E. P.; Kent, T. A.; Lindahl, P. A.; Münck, E.; Orme-Johnson, W. H. Roder, H.; Roy, A. *Biophys. J.* **1987**, *52*, 837-853.